

PICTORIAL REPRESENTATIONS OF THE ELECTRON  
CLOUD FOR HYDROGEN-LIKE ATOMS

BY H. E. WHITE

UNIVERSITY OF CALIFORNIA, BERKELEY

(Received April 21, 1931)

ABSTRACT

It is well known that the solutions of the wave-equation for hydrogen-like atoms may be represented graphically by interpreting  $\Psi\Psi^*$  as a *probability density*. The *probability density factors*  $\Phi_m\Phi_m^* \cdot [\Theta_{m,l}]^2 \cdot [R_{n,l}]^2 = \Psi\Psi^*$  are represented graphically and briefly discussed and compared with the electron orbits of four classical models. Graphs for *s*, *p*, *d*, *f*, *g*, and *h* electrons are given. An attempt to combine the *probability density factors* and form some graphical representation of  $\Psi\Psi^*$  has resulted in the construction of a mechanical device or model, see Fig. 5, which when photographed, gives very closely the desired result. Photographs for the magnetic states  $m=0, \pm 1, \pm 2, \pm 3, \dots$  are given for 1*s*, 2*p*, 3*d*, 4*f*, 2*s*, 3*p*, 4*d*, 5*f*, 3*s*, 4*p*, and 5*d* electrons, see Fig. 6.

WITH all of the successes of the quantum mechanics one still hears on every hand, for want of an atomic model, the terms *electron orbits*, *penetrating orbits*, *non-penetrating orbits*, etc. This is of course due to the fact that in many cases one may think in terms of the simpler electron orbits and be led to a result which is the same or very nearly the same as that given by the quantum mechanics. In going over some of the correlations very often made between the two theories several interesting graphical comparisons have been forthcoming.

It is well known that for a non-relativistic, conservative dynamical system of one nucleus and one electron (that is a hydrogen-like atom) Schroedinger's wave-equation

$$\Delta^2\Psi + \frac{8\pi^2\mu}{h^2}(W - V)\Psi = 0 \quad (1)$$

expressed in polar coordinates  $\phi$ ,  $\theta$ , and  $r$ , see Fig. 1 may be solved by replacing  $\Psi$  by the product of a function of  $\phi$  alone, another of  $\theta$  alone, and another of  $r$  alone,

$$\Psi = \Phi_m \cdot \Theta_{m,l} \cdot R_{n,l}. \quad (2)$$

With this substitution the equation is separated into three total differential equations the well-known solutions of which are,

$$\Phi_m = (2\pi)^{-1/2} e^{im\phi}, \quad m = 0, \pm 1, \pm 2, \pm 3, \dots \pm l \quad (3)$$

$$\Theta_{m,l} = \left( \frac{(2l+1)(l-m)!}{2(l+m)!} \right)^{1/2} \sin^m \theta \cdot P_l^m(\cos \theta), \quad l = 0, 1, 2, 3, \dots (n-1) \quad (4)$$

$$R_{n,l} = \left[ \frac{4(n-l-1)!Z^3}{[(n+l)!]^3 n^4 a_1^3} \right]^{1/2} \left( \frac{2Zr}{na_1} \right)^l e^{-Zr/na_1} L_{n+l}^{2l+1} \left( \frac{2Zr}{na_1} \right), \quad n = 1, 2, 3, \dots \quad (5)$$

involving in addition to the *normalizing factors*, the complex exponentials  $e^{im\phi}$ , the “*associated Legendre polynomials*,” and derivatives of the “*Laguerre polynomials*,” where  $m$ ,  $l$ , and  $n$ , are to be associated with the *magnetic*, *azimuthal*, and *total quantum numbers* respectively. It is also well known that  $\Psi\Psi^*dv$ , which is interpreted as the *probability* of the electrons being found in a given element of volume  $dv$  is very small outside the region occupied by the corresponding classical electron orbits.

For descriptive purposes it has been convenient to think of the *probability density*  $\Psi\Psi^* = P$  in terms of the angles  $\phi$  and  $\theta$  and of the distance  $r$  independently. From Eqs. (2), (3), (4), and (5) the *probability density*

$$\Psi\Psi^* = \Phi_m\Phi_m^* \cdot [\Theta_{m,l}]^2 \cdot [R_{n,l}]^2. \tag{6}$$

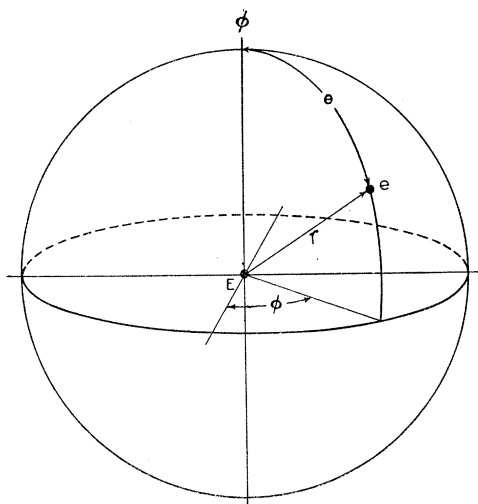


Fig. 1.

There are in general four classical models to be compared with these *probability density factors*. These four well-known models, which will here be called (a), (b), (c), and (d), have the same *total quantum number n*, and *azimuthal quantum numbers* as follows; (a)  $l$  (b)  $[l(l+1)]^{1/2}$  (c)  $l + \frac{1}{2}$ , (d)  $l + 1 = k$ . It should be pointed out that none of these classical orbital models is correct and that, for want of an atomic model, any one of them may, with certain limitations, be used. In general (a) and (b) serve as vector models while (c) and (d) serve well as orbital models.

**The  $\Phi_m\Phi_m^*$  factor.** For given  $m$ ,  $\Phi_m$  times its complex conjugate  $\Phi_m^*$  is a constant, so that for any given state the probability of an electrons being found in any small element of angle  $d\phi_1$  is the same as for any other equal angle  $d\phi_2$ . For all allowed electron states the *probability density* is therefore symmetrical about the  $\phi$  (magnetic) axis.  $\Phi_m\Phi_m^*$  plotted as a function of the angle  $\phi$  (0 to  $2\pi$ ) would graphically be represented in rectangular coordinates by a straight line or in angular coordinates by a circle.

**The  $[\Theta_{m,l}]^2$  factor.** For given  $m$  and  $l$  values the polynomials of Eq. 4 and consequently  $[\Theta_{m,l}]^2$  are readily calculated from well known recursion formulas.<sup>1</sup>

Values of the *probability density factor*  $[\Theta_{m,l}]^2$  are given in Table I and plotted in rectangular coordinates in Fig. 2.

Unsold<sup>2</sup> has shown that for given  $n$  and  $l$ , the *probability density* summed over the states  $m = +l$  to  $m = -l$  presents spherical symmetry about the nucleus. Since  $\Phi_m \Phi_m^*$  is constant for any state one has simply to show that

$$\sum_{m=-l}^{m=+l} [\Theta_{m,l}]^2 = \text{constant}. \quad (7)$$

This well-known theorem is seen to be true from the last column of Table I or graphically from the curves of Fig. 2. For example, the sum of the three

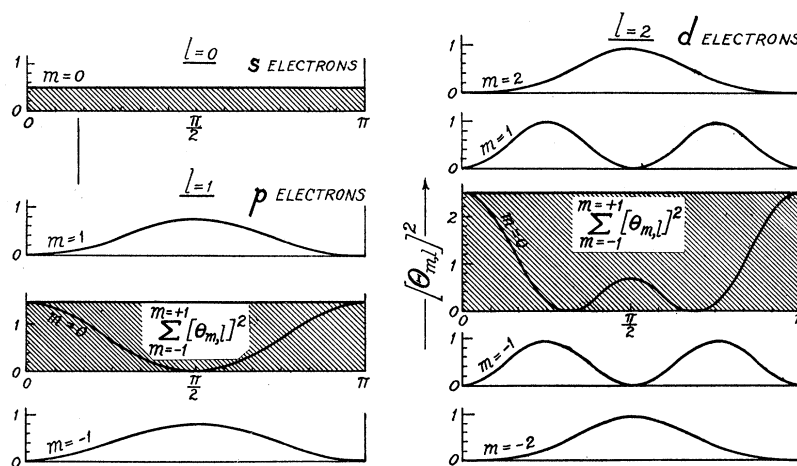


Fig. 2. The probability density factor  $(\Theta_{m,l})^2$  as a function of  $\theta$  for  $s$ ,  $p$ , and  $d$  electrons. The straight lines and the shaded areas represent spherical symmetry, the result of the summation of the curves from  $m = +l$  to  $m = -l$ .

curves for the three  $p$  states  $m = 1, 0, -1$  gives a straight line as indicated by The shaded area. Thus it is that in some of the complex spectra three similar  $p$  electrons five similar  $d$  electrons, or seven similar  $f$  electrons form spherical symmetry, that is an  $S$  term, as the most stable state.

If angular coordinates are used when plotting  $[\Theta_{m,l}]^2$  a number of interesting correlations with the classical orbits may be made. Such curves are shown in Fig. 3 for  $s$ ,  $p$ ,  $d$ ,  $f$ ,  $g$ , and  $h$  electrons. Beneath each figure the corresponding classical orbit is given oriented in each case according to the vector model (a). In order to illustrate an orbit rather than its straight line projection the  $\phi$  axis is tipped slightly out of the plane of the paper. It must be remembered that the electron is not confined to the shaded area in each

<sup>1</sup> See "Quantum Mechanics," by Condon and Morse, p. 63.

<sup>2</sup> Unsold, Ann. d. Physik **82**, 379 (1927).

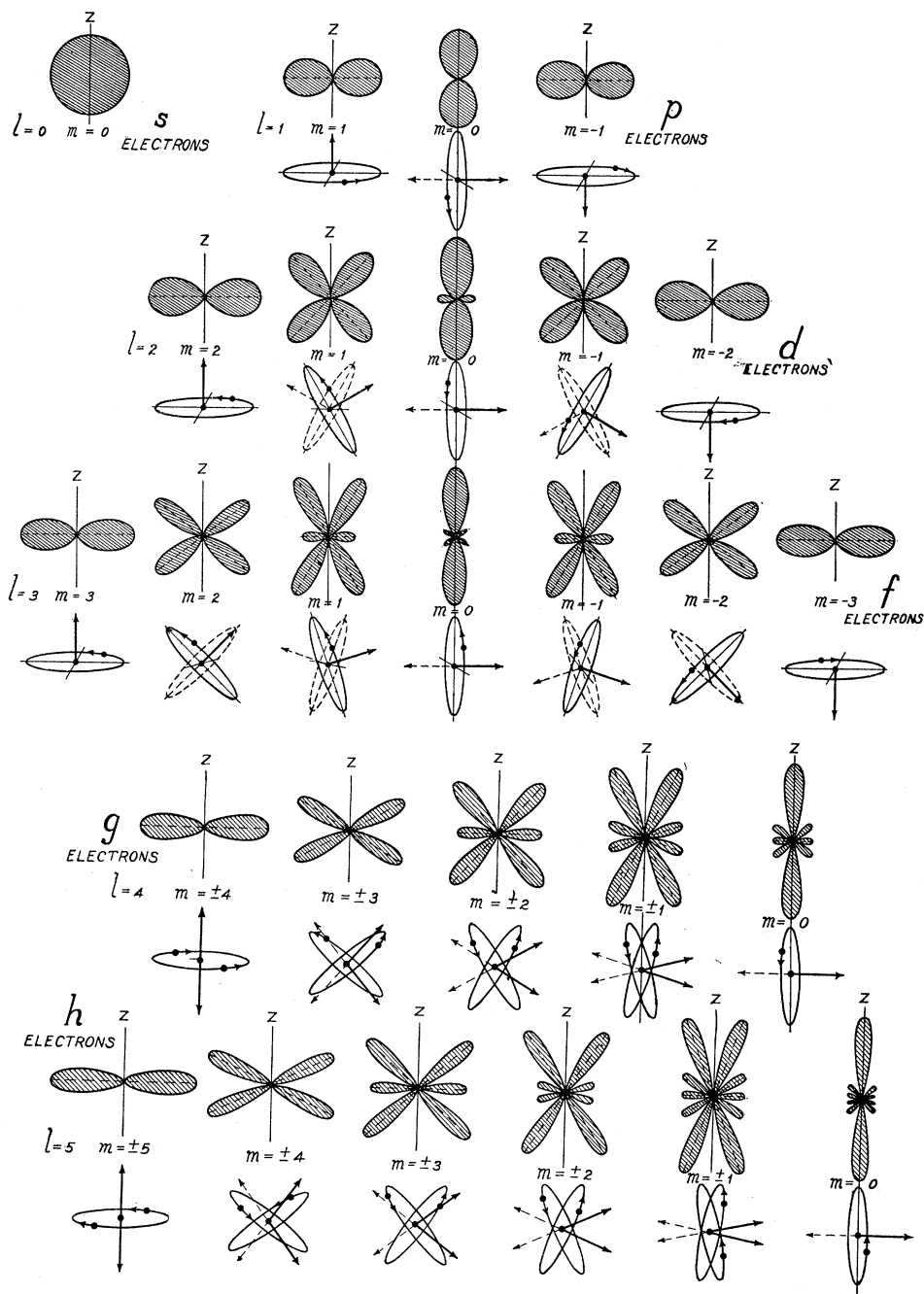


Fig. 3. The probability density factor  $(\Theta_{m,l})^2$  plotted in angular coordinates for s, p, d, f, g, and h electrons. For states  $m=0$  the scale is approximately  $1/l+1$  times that of the other states of the same  $l$  value. The classical oriented orbit for each quantum state is given below each figure, tilted slightly out of the normal plane to show an orbit rather than a straight line.

TABLE I. The probability density factor  $[\Theta_{m,l}]^2$ .

Electron	$l$	$m$	$[\Theta_{m,l}]^2$	$\sum_{m=-l}^{m=+l} [\Theta_{m,l}]^2$
$s$	0	0	1/2	1/2
$p$	1	$\pm 1$	$3/4 \sin^2\theta$	3/2
		0	$3/2 \cos^2\theta$	
$d$	2	$\pm 2$	$15/16 \sin^4\theta$	5/2
		$\pm 1$	$15/4 \sin^2\theta \cos^2\theta$	
		0	$10/16 (3 \cos^2\theta - 1)^2$	
$f$	3	$\pm 3$	$35/32 \sin^6\theta$	7/2
		$\pm 2$	$105/16 \sin^4\theta \cos^2\theta$	
		$\pm 1$	$21/32 \sin^2\theta (5 \cos^2\theta - 1)^2$	
		0	$7/8 (5 \cos^3\theta - 3 \cos \theta)^2$	

probability figure but that the magnitude of a line joining the center and any point on the curve is a measure of the electrons probability of being found in the direction of that line.

Since the plane in which each curve is drawn represents any plane through the  $\phi$  axis symmetry of  $\Phi_m \Phi_m^*$  is obtained by rotating each curve about the  $\phi$  (or *magnetic*) axis. Corresponding to this axial symmetry there is the classical precession of each orbit around the  $\phi$  axis producing a somewhat similar figure. For each  $m=0$  curve the scale used is about  $1/l+1$  times that of the other curves of the same  $l$  value.

For all  $m=0$  states, excluding the spherically symmetrical  $s$  states, the *probability density* is greatest in the direction of the poles. With the exponent of  $e^{im\phi}$  zero this distribution has been interpreted to mean<sup>3</sup> that there is no motion in the  $\phi$  coordinate and that correlated with this the motion of the electron (i.e. the orbital plane) is in some one meridian plane, all meridian planes being of equal probability. The end states  $m = \pm l$  on the other hand take on their largest values in the direction of the equatorial plane. In this case one correlates the opposite signs in the exponents of  $e^{\pm im\phi}$  with the opposite directions of rotation in the orbit. The way in which each classically oriented orbit follows the corresponding curves, from  $m = +l$  to  $m = -l$ , especially for the states of higher  $l$  value, is quite remarkable. It should be mentioned that if the classical orbits are oriented according to models (b), (c), or (d) that their general agreement with the probability curves is not as good as with model (a), however, this may be a matter of personal opinion.

**The  $[R_{n,l}]^2$  factor.** The factor  $[R_{n,l}]^2$  which gives the *probability density* as a function of  $r$  alone has been discussed in detail by many investigators. For given values of  $n$  and  $l$  the Laguerre polynomials and hence  $R_{n,l}$  (see Eq. (5)) and  $[R_{n,l}]^2$  may be evaluated.<sup>1</sup> Plotting  $[R_{n,l}]^2$  against  $r$  in units of the radius of the first Bohr circular orbit  $a^1 = 0.528$  AU. give the heavy line curves of Fig. 4. Multiplying  $[R_{n,l}]^2$  by  $4\pi r^2$ , the area of a sphere of radius  $r$ , one obtains the so called *probability density distribution* curves,  $D$ , indicated by the shaded areas in the figure. The classical orbits corresponding to each of these

<sup>3</sup> See, Condon and Morse, "Quantum Mechanics."

curves, using model (c), are also shown. In each curve the *density distribution* differs greatly from zero only within the electron-nuclear distance of the corresponding classical orbits.

A more satisfactory correlation has been made by Pauling<sup>4</sup> by comparing the average value of  $r$  as calculated on both theories. The method of evaluating  $r$  from the quantum mechanics has been given by Waller<sup>5</sup> and is identical with the value obtained for the classical orbits if the *azimuthal quantum number* is taken to be  $[l(l+1)]^{1/2}$ , model (b). This average value of  $r$  is indicated in

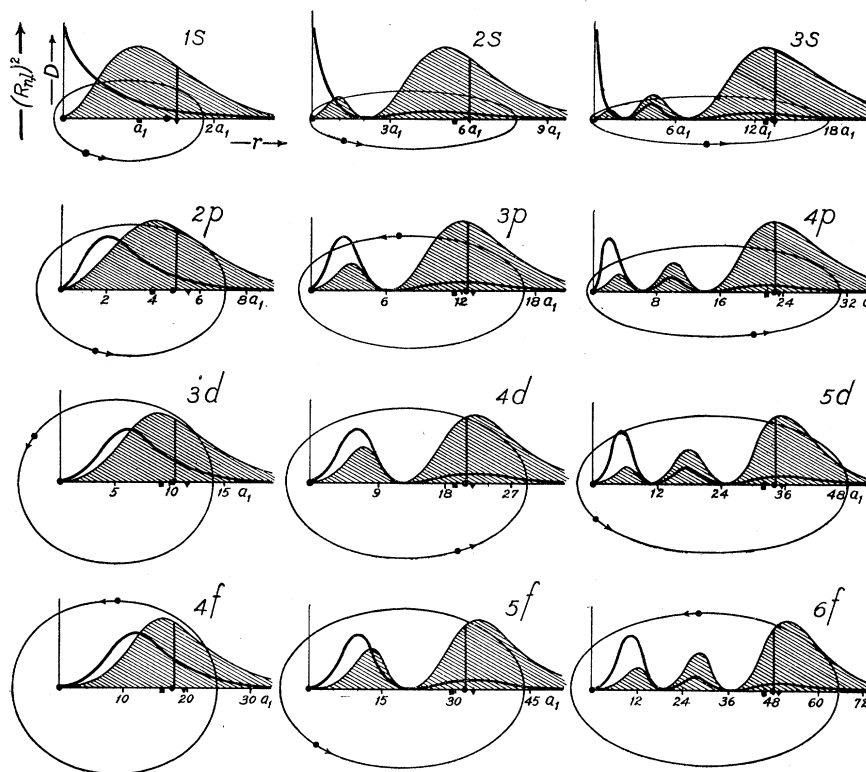


Fig. 4. The probability density factor  $(R_{n,l})^2$  plotted as a function of the electron-nucleus distance  $r$  ( $r$  is measured in units of the first Bohr circular orbit). The density distribution curves  $D = 4\pi r^2 \cdot (R_{n,l})^2$  the shaded areas, are to be compared with the electron-nucleus distance for the classical orbits, where the azimuthal quantum number is taken to be  $l + \frac{1}{2}$ .

each curve by a vertical line. The average value of  $r$  calculated for models (a), (c), and (d) are indicated on the  $r$  axis by triangular, circular, and square dots respectively.

For this radial comparison model (b) is to be preferred, however, a difficulty arises for the  $s$  states where the orbits reduce to straight lines with one

<sup>4</sup> Pauling, Proc. Roy. Soc. 114, 181 (1927).

<sup>5</sup> Waller, Zeits. f. Physik 38, 635 (1926).

end at the nucleus center. With model (c), the orbits shown in the figure, this difficulty does not arise and the agreement is practically the same.

#### THE PROBABILITY DENSITY $\Psi\Psi^*$

Attempts to bring together the *probability density factors*  $\Phi_m\Phi_m^*$ ,  $[\Theta_{m,l}]^2$ , and  $[R_{n,l}]^2$  into one single picture for  $\Psi\Psi^*$ , if we may call it a picture, have been somewhat successful. Langer and Walker<sup>6</sup> using a method which is as yet unpublished, have produced *probability density* photographs which represent the spherically symmetrical *s* states and the *2p* states  $m = +1$  and 0.

Preliminary attempts to produce a three dimensional model which will represent as closely as possible the *probability density*  $\Psi\Psi^*$  has resulted in a mechanical device shown in Fig. 5. Spindles like the one shown in the center

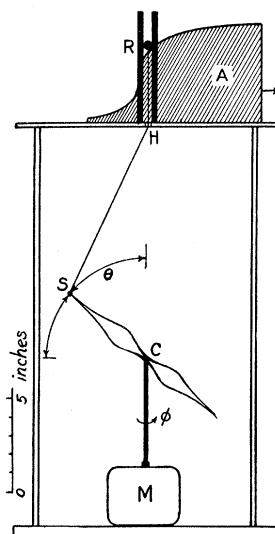


Fig. 5. A mechanical device which when set in motion and photographed represents the electron cloud for the various states of the hydrogen-like atoms. The model shown in the figure is for a  $3d$  electron.

of the figure and in the last photograph of Fig. 6 are turned out on a lathe so that in projection they give the *density distribution*  $D$  curves of Fig. 4. Such a spindle is pivoted at its center by a small pin at  $C$ , and set in rotation about the vertical axis by means of a motor  $M$ . This motion gives the required symmetry about  $\phi$ . At the same time that rotation about the  $\phi$  axis is taking place, the angle  $\theta$  is changed slowly from  $\theta = 0$  to  $\theta = \pi/2$  by means of a swivel  $S$  and a double cord  $SHR$  which passes through a hole in the table top to a roller  $R$ , the motion of which is confined to the slot as shown. Curves of thin wood, e.g.  $A$  in Fig. 5, are cut so that when they are moved slowly but with uniform speed along the table top in the direction indicated by the arrow the angular

<sup>6</sup> See, "Atoms Molecules and Quanta," by Ruark and Urey, p. 565. Also Slater, *Phys. Rev.* 37, 482 (1931).

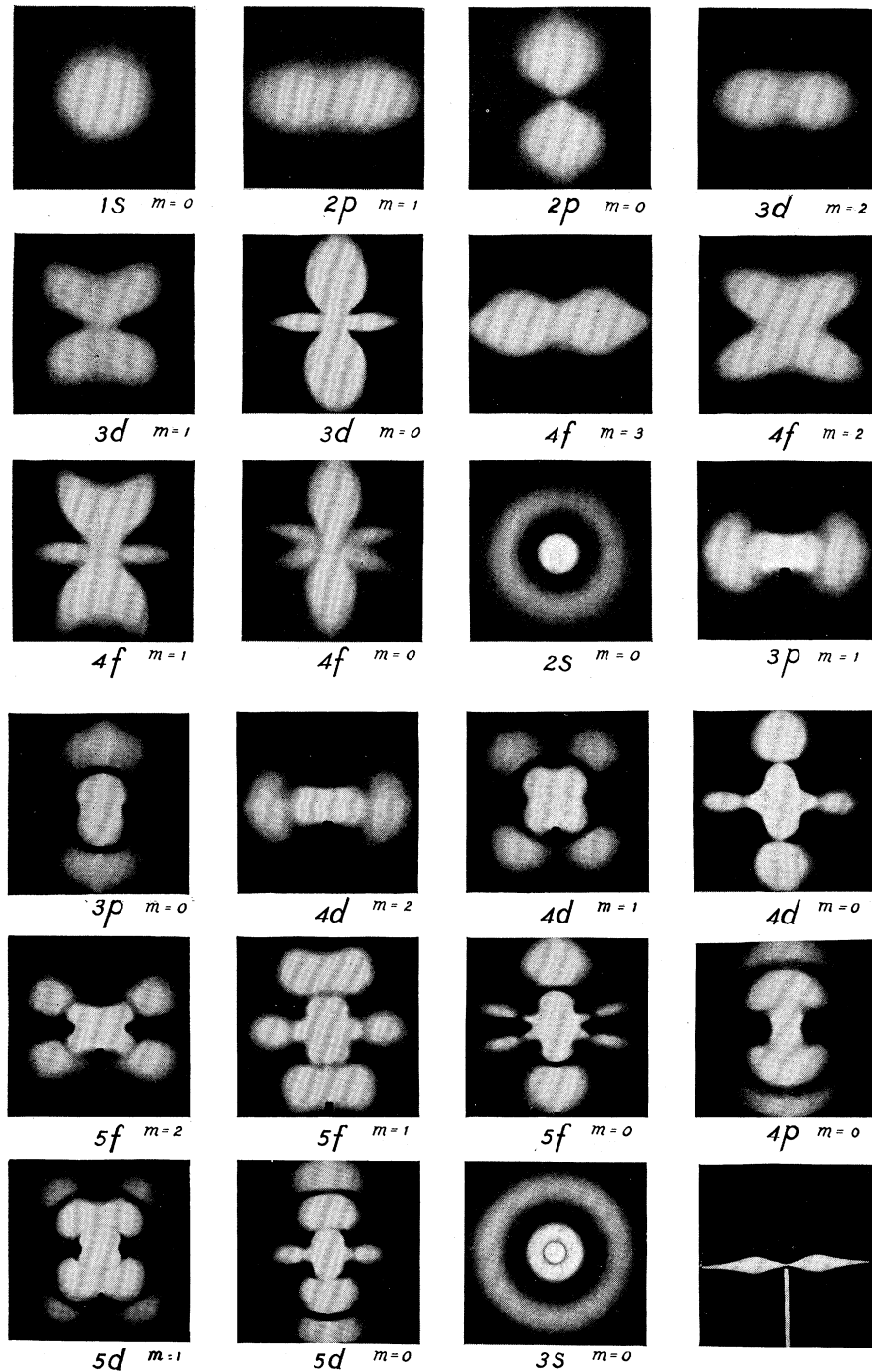


Fig. 6. Photographs of the electron cloud for various states of the hydrogen-like atoms as obtained from various models and the device shown in Fig. 5. The probability density  $\Psi\Psi^*$  is symmetrical about the  $\phi$  or magnetic axis which is vertical. The scale for each figure may be obtained from Fig. 4.

velocity  $d\theta/dt$  is changed in the proper manner to give, as nearly as possible, the correct density when photographed. A time exposure started when  $\theta=0$  and stopped when  $\theta=\pi/2$  for the model shown yields the figure for the  $3d$  state  $m=0$ . In constructing the various curves to be used at  $A$ , the changing angle of the cord  $HR$  was taken into account and also the fact that as  $\theta$  increases each point on the spindle moves in larger and larger circles and therefore faster. A small slot milled in the lower half of each spindle allows the angle  $\theta=0$  to be reached. In projection each spindle should represent the *density distribution* curves,  $D$  of Fig. 5, in order that when rotating simultaneously about the  $\phi$  and  $\theta$  axes they give at each point in space the *density*  $[R_{n,l}]^2$  curves of Fig. 5. It should be pointed out that there is a small amount of distortion due to the end on view of the spindle. This distortion is quite negligible, however, in that in this position the rapid motion as seen from the camera effects the photographic plates but little. Photographs for the states with negative  $m$  values are identical with those of positive  $m$  values. It may be seen by an examination of the figures that the addition of the  $2p$  states  $m=1, 0, -1$  or the sum of the  $3d$  states  $m=2, 1, 0, -1, -2$  will give spherical symmetry a figure like that of a  $1s$  electron. Again the summation of the  $4d$  states  $m=2, 1, 0, -1, -2$  will give spherical symmetry resembling the  $2s$  state. This may be considered as somewhat of a check on the figures in general and is quite as good as can be expected both from the standpoint of photographic reproduction of densities and the mechanical difficulties in the model.

The  $s$  states in Fig. 6 were made in a much simpler manner than the others and represent cross-sections only. Curves cut from white paper glued to the face of a blackened disk, and set rotating give the figures shown. Cross-section photographs have also been made for the nodal states by changing  $\theta$  alone,  $\phi$  remaining fixed. While these photographs are in general better, the more complete three dimensional reproductions are given in Fig. 6. The author wishes to take this opportunity to thank Professor Oppenheimer for his criticism of this paper.

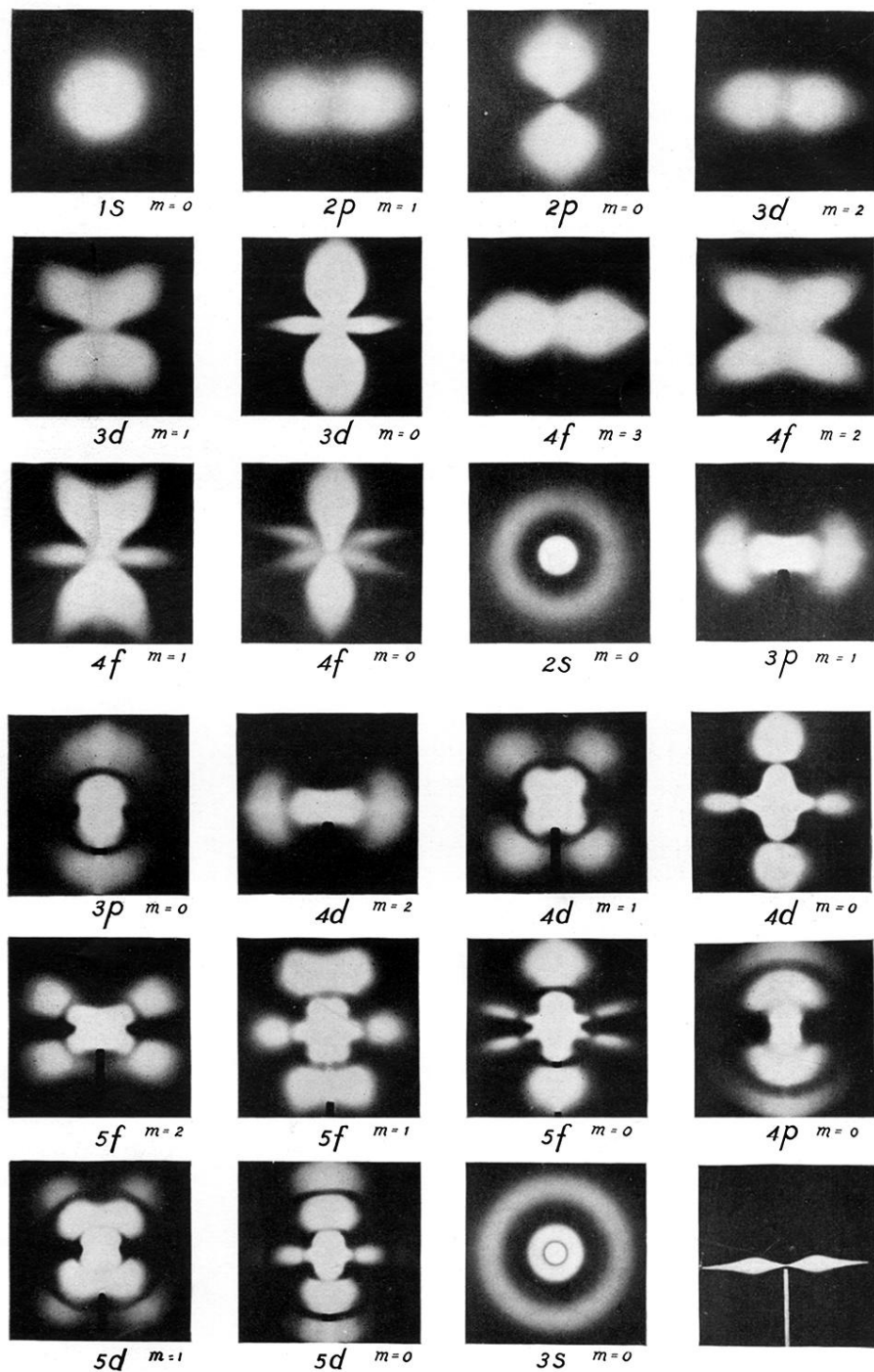


Fig. 6. Photographs of the electron cloud for various states of the hydrogen-like atoms as obtained from various models and the device shown in Fig. 5. The probability density  $\Psi\Psi^*$  is symmetrical about the  $\phi$  or magnetic axis which is vertical. The scale for each figure may be obtained from Fig. 4.